

Thick Blending-Stacking-Layer Carbon Nanotube Cathode with Improved Stability and Balanced Electron Emission: Design Optimization and Experimental Fabrication

LI Yu-kui*, WANG Wen-xiu, YANG Juan

School of electronic information engineering, Jinling Institute of Technology, Nanjing 211169, P. R. China

*Corresponding Author.

Abstract

A novel carbon nanotube cathode was designed and fabricated on cathode substrate-glass, which mitigated the topical problem of poor electron emission properties of screen-printed carbon nanotube cathodes. The fabrication for the stacking-layer structure of emitter-monolayer/ SiO₂-mixing-layer/ bottom-bar-electrode was adopted, and the preparation process of repeated printing + simultaneous sintering was employed. With this production, a higher electron emission current increase and better electron emission characteristics were obtained. When the electric field was increased from 2.199 to 2.877V/ μm , the electron emission current was enhanced from the initial 299.7 to 2125.6 μA (i.e., by more than seven times), gaining the electron emission increase of 1825.9 μA . The fabricated cathode exhibited a large electron emission current and a low turn-on electric field: the electric field required for achieving the electron emission current of 988.2 μA was only 2.623V/ μm . Moreover, it possessed stable electron emission and high emission current measuring repeatability. The uniform luminescent image with high brightness was realized, which proved that the proposed thick blending-stacking-layer carbon nanotube cathode had a balanced electron emission current.

Keywords: screen-printed cathode, balanced electron emission, blending, repeated printing, sintering

1. Introduction

carbon nanotubes (cnts) possess excellent electron emission capability due to their unique properties, such as preferable electrical conductivity, high chemical stability, and extremely high mechanical strength [1-3]. with the screen-printing method, the cnt film can be prepared to form a cold electron source of backlight units, in which the emitted electrons from the cnt cathode would accumulate and contribute to the cathode current [4-6]. the screen-printing method is quite lucrative for cathode preparation due to its low cost, large-area fabrication, and pattern cathode manufacturing [7-9]. however, screen-printed cnt cathodes' electron emission properties are strongly deteriorated by the random distribution of cnts [10-12]. alternatively, cnt films prepared via chemical vapor deposition process have the advantages of good substrate contact, uniform cnts array, and excellent electron emission performance, but control of their large-area preparation conditions is quite problematic [13-15]. the cnt films prepared with electrophoretic deposition technique have high film-forming quality and operate at room temperature. still, the unreliable connection between the formed cnt film and the substrate restricts their mass production [16-18]. adhesive taping and mechanical rubbing are effective methods to obtain larger emission currents by removing the residual material covering the surface of screen-printed cnt film, but their application is accompanied by the secondary contamination and mechanical damage of thus treated cnt films [19-21]. given this, a new thick blending-stacking-layer (tbsl) cnt cathode was fabricated in this study, which adopted a stacking-layer fabrication of emitter-monolayer/ sio₂-mixing-layer/ bottom-bar-electrode structure and the preparation process of repeated printing + simultaneous sintering. the fabricated tbsl cnt cathode exhibited improved electron emission characteristics, enhanced emission current stability, and measuring repeatability. its application produced a luminescent image with good uniformity and high brightness.

2. Experimental

2.1. Cathode structure and printing pastes

A TBSL CNT cathode with an emitter-monolayer/ SiO₂-mixing-layer/ bottom-bar-electrode stacking layer structure

was designed in this study. Its structural diagram is shown in Fig.1. Cathode substrate-glass, made of flat sodium-calcium glass, provided the supporting substrate for the TBSL CNT cathode.

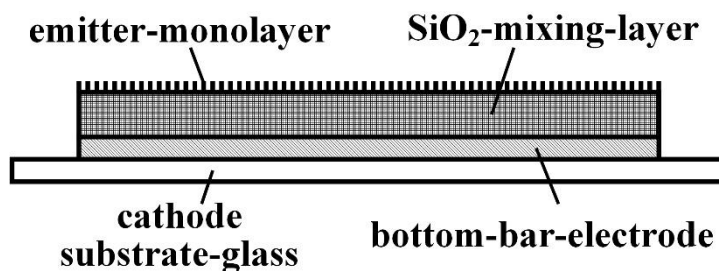


Fig.1. Structural diagram of the TBSL CNT cathode

Two types of cathode printing pastes, namely the emitter-monolayer paste and SiO₂-mixing-layer paste, were prepared in advance. For SiO₂-mixing-layer paste, the multi-walled CNT/graphene aqueous slurry of purity exceeding 90wt% was mixed with SiO₂ particles, terpineol, and a small amount of other organic solvents. The mixture was blended in a beaker at room temperature and then placed into an electromagnetic stirrer, where it was heated to the maximum temperature of 115°C. This temperature was maintained constant during a stirring process until a smooth SiO₂-mixing-layer paste was prepared. For emitter-monolayer paste, the multi-walled CNT, ethylcellulose, terpineol, and tiny amounts of other organic solvents were blended in another beaker to constitute the emitter-monolayer mixture. The heating and stirring processes, which were identical to the above-mentioned ones for the SiO₂-mixing-layer paste, continued until a viscous and uniform emitter-monolayer paste was formed.

2.2. Cathode fabrication

In this experiment, firstly, the silver slurry was screen-printed onto cathode substrate-glass to form the bottom-bar-electrode. Secondly, the repeated-printing preparation course was performed: the SiO₂-mixing-layer paste was screen-printed onto the bottom-bar-electrode, and a baking process was conducted in the automatic electric oven. The baked SiO₂-mixing-layer paste was used to constitute the first sub-SiO₂-mixing-layer. The SiO₂-mixing-layer paste was printed over the latter. After the second baking process, the two sub-SiO₂-mixing-layer layers were fabricated. Both baking process parameters were identical: the employed equipment was an automatic electric oven, the maximum baking temperatures was 192°C, the baking time was approximately 25 min, and the baking environment was the atmosphere. Subsequently, in a sintering furnace, the simultaneous sintering process was conducted for both sub-SiO₂-mixing-layers. The corresponding sintering process parameters included a maximum sintering temperature of 537°C, the maintaining time at the maximum sintering temperature of 4.5min, nitrogen as a shielding gas, and the total sintering time of approximately 60 min. Thus, the SiO₂-mixing-layer was fabricated on the bottom-bar-electrode. Then, the emitter-monolayer paste was screen-printed onto the sintered SiO₂-mixing-layer. The corresponding baking and sintering processes were then carried out in the proper sequence, so the emitter-monolayer was fabricated. The partial process parameters were adjusted for the baking and sintering processes as follows: a baking temperature of 235°C, a baking time of 20 min, a maximum sintering temperature of 516°C, a maintaining time at the maximum sintering temperature of 6.5 min, and argon as a shielding gas. Next, a proper post-treatment process was applied to the sintered emitter-monolayer, finalizing the TBSL CNT cathode fabrication. For comparison, the conducting electrode CNT cathode was also fabricated, in which the emitter-monolayer was prepared directly onto the bottom-bar-electrode.

3. Results and discussion

3.1. Surface topography photos

The surface morphology photos are presented in Fig.2(a-d). The employed equipment was a scanning electron microscope (SEM). The analyzed samples comprised two fabricated types of CNT cathode. In the analyzing course, the magnification multiples were adjusted.

The surface morphology of the baked TBSL CNT cathode is shown in Fig.2(a). As shown in Fig.2, the emitter-monolayer surface still contained numerous organic slurry blocks, and the distribution of organic slurry blocks was also irregular. The analysis revealed the following issues. (1) The baking process involved low baking temperature. With the given baking temperature, the partial organic adhesive materials could be removed with the

baking process. Once the partial organic adhesive materials were disposed of, the organic slurry blocks also disappeared. However, all organic adhesive materials could not be eliminated only by the baking process. In the experimental process, the maximum baking temperature should be limited by the bearing capacity of practical baking equipment. If the baking temperature is too high, the test baking equipment might be damaged and even destroyed. For further processing, the sintering process is considered the best option. (2) The organic slurry blocks contained many hydrous ingredients, which might have two possible harmful effects. The first one is the critical reduction of the backlight sample's inner vacuum degree. The second one is the short circuit between the different bar cathodes. Consequently, the organic slurry blocks should be removed as thoroughly as possible. Fig.2(b) shows the surface morphology of sintered TBSL CNT cathode, with a magnification of 30000. As can be seen, a flat, clean, and smooth emitter-monolayer film surface appeared. The performed analysis of the above morphology revealed the following patterns. (1) Due to organic slurry blocks, many CNTs would be reunited; thus, the emitter-monolayer film surface was rugged. In the sintering course, many organic slurry blocks were evaporated and disappeared. The original CNT film surface was also recovered, so a flat emitter-monolayer film surface certainly appeared. This resulted in a more uniform electric field distribution, so more CNT ends could be forced to emit electrons simultaneously, which is beneficial to enhance the luminescence brightness of the backlight sample. (2) As seen from Fig.2, there were no other impurities on the emitter-monolayer film surface, except for the random-distributed CNTs. A clear emitter-monolayer film surface ensured that cathode electrons could be emitted only by CNTs in the formed cathode current, so other impurities could not contribute to the emission of cathode electrons. For this reason, CNTs could endure a high sintering temperature (e.g., 516°C) and would not be evaporated in the sintering course. On the other hands, due to the shielding gas (for example, argon) protection, CNTs would not be oxidized or transformed into other impurities. (3) CNTs in the emitter-monolayer were intertwined, and the whole distribution was uniform, so a smooth emitter-monolayer film surface was obtained. Due to the mutual constraints among different CNTs, their firmness in the TBSL CNT cathode would be greatly enhanced. Even under strong electric field action, the CNTs in emitter-monolayer films would not fall off easily. This allows one to avoid several unfavorable phenomena, such as the backlight sample destruction by the cathode-grid short circuit or the abnormal image of the TBSL CNT cathode due to the interference of different CNTs.

The SEM photo of sintered conducting electrode CNT cathode is presented in Fig.2(c), with a magnification of 30000. The comparative analysis of Fig.2(b) and Fig.2(c) revealed that, after the sintering process, the conducting electrode CNT cathode also possessed a cathode surface similar to that of the TBSL CNT cathode. The performed sequential baking and sintering processes effectively removed the organic slurry blocks. The organic slurry blocks would be directly evaporated in the sintering course because they could not bear such a high sintering temperature, yielding a clear emitter-monolayer film surface. Even if, in the sintering course, some organic slurry materials would be transformed into other impurities, they would be carried away by the flowing shielding gas. Thus, it ensured the formation of a pure emitter-monolayer film. The SEM photo of sintered TBSL CNT cathode is presented in Fig.2(d), with a magnification of 45000. Comparing Fig.2(b) with Fig.2(d), it can be observed that many CNT ends fully protruded through the emitter-monolayer film surface. The analysis shows that the usage of organic adhesive materials in viscous cathode printing pastes was not optimal for fabricating the patterned CNT cathode with the low-cost screen-printing method. On the contrary, once the patterned CNT cathode was prepared, the remaining organic adhesive materials would obstruct the normal electron emission of CNT ends. Therefore, these residual materials should be eliminated from the prepared CNT cathode. After the sintering process, the CNT ends should not be buried, covered, or reunited by the organic slurry blocks. As a result, the numerous protruding CNT ends could become potential electron sources in the TBSL CNT cathode. Due to the emitter-monolayer covering, the SiO₂ particles and graphene in the SiO₂-mixing-layer were invisible on the emitter-monolayer film surface.

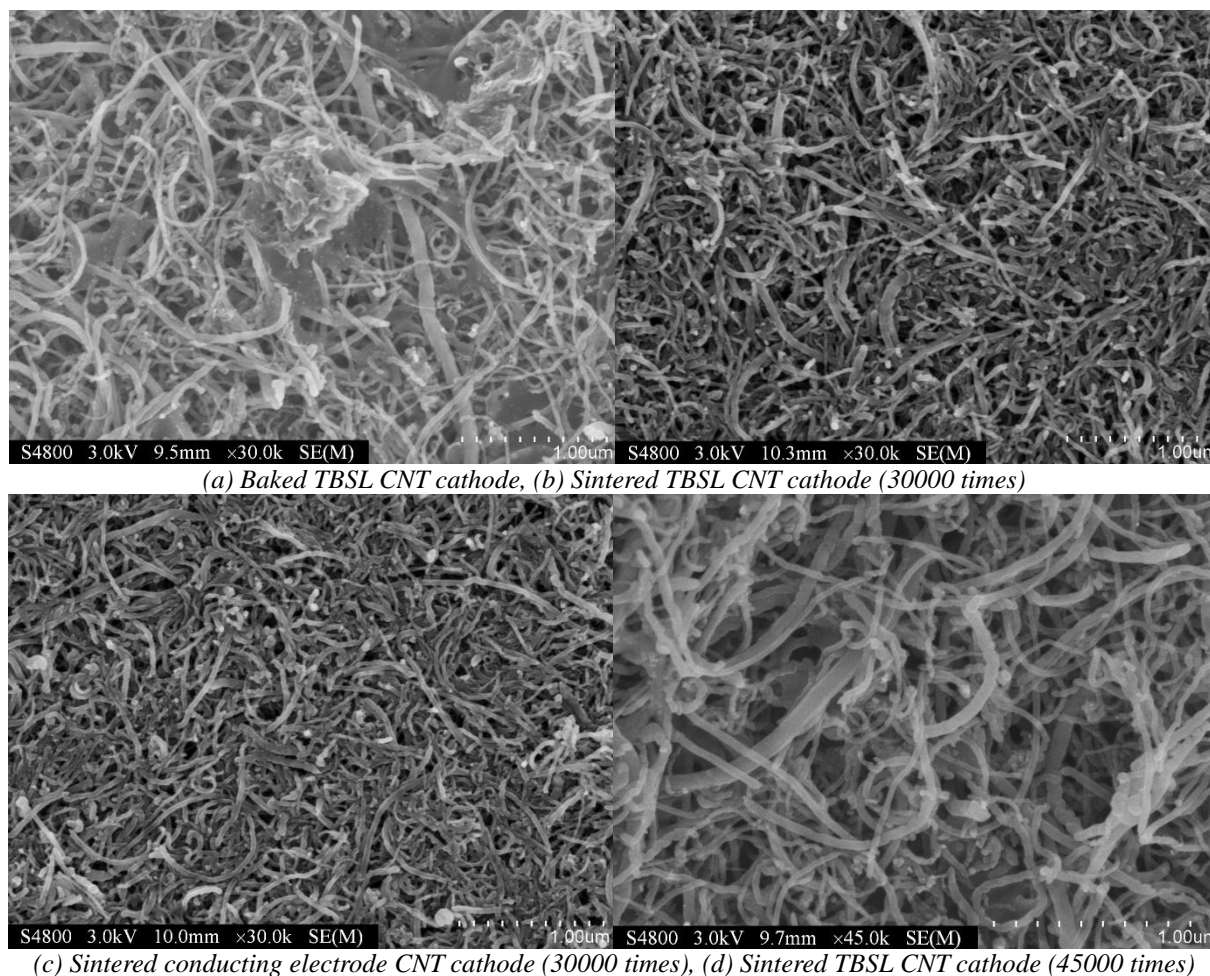


Fig.2. Surface topography photos for both types of CNT cathode

3.2. Emission characteristic curves

Electron emission characteristics are crucial for assessing the functional application performance of screen-printed CNT cathodes [22-24]. In this experiment, the electron emission characteristics were measured for the two types of CNT cathodes. The measuring conditions were as follows: the integrated vacuum testing system was employed as the testing platform; two independent direct current (DC) sources were used to apply bias voltages; the ammeter was utilized for current measuring; the system vacuum degree had the order of 10^{-4} Pa. Both types of CNT cathode were assembled into the vacuum chamber of the integrated vacuum testing system. Thus, under identical measuring conditions, the characteristic emission curves for the two types of CNT cathodes were plotted, as shown in Fig.3.

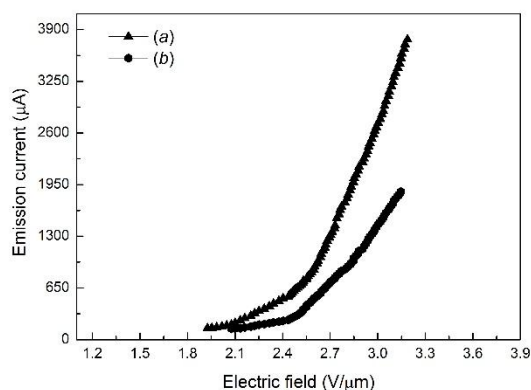


Fig.3. Emission characteristic curves for (a) TBSL CNT cathode and (b) conducting electrode CNT cathode

As shown in Fig.3., both types of CNT cathodes could supply cathode electrons. However, the TBSL CNT cathode had a higher electron emission current increase and better electron emission characteristics. For example, when the electric field was increased from 2.199 to 2.877V/μm, the electron emission current of conducting electrode CNT cathode was enhanced from the initial 164.3 to 1083.7μA, yielding the electron emission increase of 919.4μA. Meanwhile, the TBSL CNT cathode enhanced the electron emission current the initial 299.7 to 2125.6μA, gaining the electron emission increase of 1825.9μA and exceeding that of the former cathode by 906.5μA. The manufacturing process involved the repeated-printing + simultaneous sintering preparing method in the TBSL CNT cathode fabrication course, as follows. The first baked SiO₂-mixing-layer paste was used to fabricate the first sub-SiO₂-mixing-layer. Then, the SiO₂-mixing-layer paste was printed and baked onto one sub-SiO₂-mixing-layer to constitute the second sub-SiO₂-mixing-layer. Both sub-SiO₂-mixing-layers were simultaneously sintered in a sintering furnace, forming the SiO₂-mixing-layer with a large thickness. For the TBSL CNT cathode, the SiO₂-mixing-layer was sandwiched between the emitter-monolayer and the bottom-bar-electrode, while the SiO₂-mixing-layer contained a large amount of graphene. Because the CNT and graphene had similar functionality, they easily form a good ohmic contact. Moreover, the graphene's conducting capability was improved, and the carrier mobility in graphene was enhanced. As a result, the stacking-layer structure with emitter-monolayer/SiO₂-mixing-layer/ bottom-bar-electrode possessed superior electrical conductivity. Using the SiO₂-mixing-layer as an intermediate transition layer, the impedance between the bottom-bar-electrode and emitter-monolayer could be further reduced, and the electron mobility would be improved effectively. As seen from the measuring curves, cathode currents could be produced by both types of CNT cathodes. Thus, cathode electrons could be properly transmitted by the bottom-bar-electrode in the conducting electrode CNT cathode and the stacking-layer structure of emitter-monolayer/ SiO₂-mixing-layer/ bottom-bar-electrode in the TBSL CNT cathode. However, the electric potential transferability of the latter was better, so a stronger electric field could be quickly formed on the emitter-monolayer film surface. This field would force CNT ends in the emitter-monolayer of the TBSL CNT cathode to emit electrons, which would accumulate and contribute to the cathode current of the backlight sample. Therefore, as shown in the curve variation trend in Fig.3, with a continuous enhancement of the applied electric field, the number of cathode electrons provided by the CNT ends of the emitter-monolayer in TBSL CNT cathode would also increase significantly. Accordingly, its electron emission current increase and electron emission characteristics outperformed those of the conducting electrode CNT cathode. This is also confirmed by photos in Fig.2(b) and Fig.2(c). Both cathodes had pure and single emitter-monolayer film surfaces, and cathode electrons forming the cathode current were also derived from the as-prepared CNT ends on the emitter-monolayer. However, in the measuring course of electron emission characteristics, the achieved electron emission performance of the TBSL CNT cathode was superior. This proved that the stacking-layer structure of emitter-monolayer/SiO₂-mixing-layer/ bottom-bar-electrode in TBSL CNT cathode played an important role.

While both types of CNT cathodes could form cathode currents, the TBSL one possessed a larger electron emission current and a lower turn-on electric field. For example, at the applied electric field of 2.508V/μm, the electron emission current of conducting electrode CNT cathode was only 327.3μA, while that of TBSL exceeded it by 349.6μA, reaching 676.9μA. To achieve the same electron emission current (e.g., 988.2μA), the required electric field for the TBSL CNT cathode was 2.623V/μm, while that conducting electrode one was 2.846V/μm, i.e., higher by 0.223V/μm. The turn-on electric fields of conducting electrode and TBSL CNT cathodes were 2.077 and 1.926V/μm, respectively, differing by 0.151V/μm. The analysis shows that the SiO₂-mixing-layer of TBSL CNT

cathode contained SiO₂ particles, which appeared in the repeated-printing preparation course. In the “simultaneous sintering” process, these particles were randomly dispersed and occupied the idle space of adjacent CNTs. CNTs in the emitter-monolayer film were very easy to intertwine due to their small size, high aspect ratio, and large surface area. Due to the high thermal conductivity and abrasive resistance of the SiO₂ particles, they could rapidly diffuse a large amount of heat released in the local area due to the strong local electric field action. Thus, the CNTs could be effectively protected. Due to the high insulation performance and corrosion resistance of the SiO₂ particles, the vacuum area (that is, the idle space) between adjacent CNTs would be occupied by the supplementary SiO₂ particles, isolating the adjacent CNTs. As a result, in the emitter-monolayer, the preparation density of CNTs would be effectively reduced, and the shielding effect of the electric field would also be favorably reduced. The above factors decreased the TBSL CNT cathode’s turn-on electric field and increased its electron emission current. Moreover, the SiO₂-mixing layer also contained graphene with good electric conduction capability, so SiO₂ particles would not obstruct the high-speed transmission of cathode electrons from the bottom-bar-electrode in the SiO₂-mixing-layer to the emitter-monolayer. Besides, the discrete electron emission caused by the SiO₂ particles in the SiO₂-mixing-layer of the TBSL CNT cathode was completely suppressed by the emitter-monolayer’s covering. This is also in concert with photos of Fig.2(b) and Fig.2(d): the obtained characteristic curves do not conform with those of pure SiO₂ particles, SiO₂+CNTs mixtures, or SiO₂+graphene+CNTs mixtures. The emitter-monolayer of the TBSL CNT had a clean surface, so the effective electron emission area was greatly increased, which was beneficial for the electron emission current enhancement.

3.3. Experimental curves of emission current stability and measuring repeatability

The emission current stability and measuring repeatability of screen-printed CNT cathode are crucial for practical applications [25-27]. These characteristics of the TBSL CNT cathode are experimentally determined in this study. The test conditions were as follows. The integrated vacuum testing system was employed. The TBSL CNT cathode was installed in the vacuum chamber of the integrated vacuum testing system, with a vacuum degree of the order of 10⁻⁴Pa. Two tests on the emission current stability and emission current measuring repeatability were carried out, with an interval of 3h between them. The duration time of each test was 35 min; the interval time of current monitoring was 1 min; the electric test field was fixed at 2.696V/μm. The test conditions for the emission current stability and emission current measuring repeatability were identical. The obtained experimental curves are plotted in Fig.4.

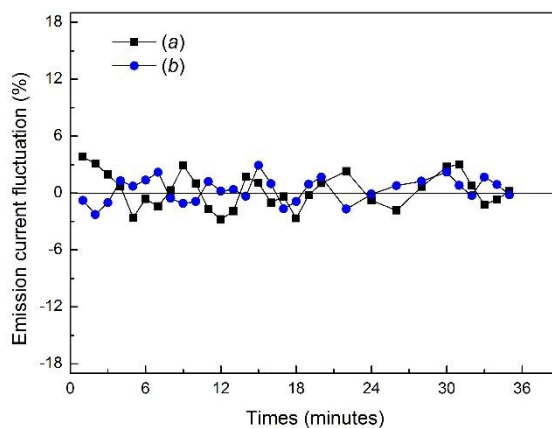


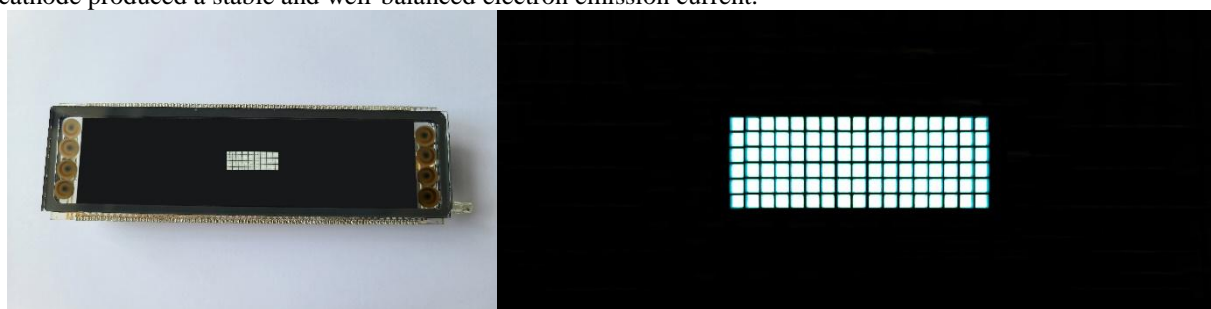
Fig.4. Experimental curves of emission current stability and emission current measuring repeatability for the TBSL CNT cathode: (a) first test, and (b) second test

As seen in Fig.4, the TBSL CNT cathode’s electron emission was stable in the whole testing course. No current variations with “big and small jumps” or current attenuations with “a steady emission, following by linear reduction” trends were observed. This indicated that the TBSL CNT cathode possessed good emission current stability. The maximum emission current fluctuation rates of the TBSL CNT cathode did not exceed 4.3 and 3.9% in the first and second tests, respectively, with a negligible difference of 0.4%. This also indicates a good emission current measuring repeatability of the TBSL CNT cathode. In the latter’s fabrication, the SiO₂-mixing-layer was sandwiched between the emitter-monolayer and the bottom-bar-electrode. On the one hand, even if the sintered bottom-bar-electrode surface was quite rough, it would be covered by the SiO₂-mixing-layer and do not affect the emitter-monolayer’s preparation quality. On the other hand, the fabricated SiO₂-mixing-layer was instrumental; in achieving a flat, clean, and smooth emitter-monolayer surface with an increased number of CNT ends. This

enhanced the electron emission current of the TBSL CNT cathode: more electrons could be simultaneously emitted from numerous CNT ends on the emitter-monolayer surface, which improved the voltage regulation capability of the TBSL CNT cathode. Moreover, in the latter's fabrication, the layer thickness of the SiO₂-mixing-layer was effectively increased by the repeated-printing preparation process. With the simultaneous sintering process, the preparation process of screen-printed CNT cathodes was simplified, and the negative effect on emitter-monolayer was also effectively mitigated.

3.4. Emission images

If the prepared CNT cathode could provide a long-term and stable cathode current for the backlight sample, its practical application value would be proved. The anode substrate-glass was fabricated with the cut flat sodium-calcium glass; the anode substrate-glass and cathode substrate-glass were combined to make a vacuum room for sealing the TBSL CNT cathode. Thus, a backlight sample with the TBSL CNT cathode was fabricated, which photo is presented in Fig.5(a). The backlight sample was rectangular; its electrodes were encapsulated in the vacuum room and connected to the output terminal with the corresponding lead wire. The normal luminescence of the backlight sample could be achieved after proper bias voltage was applied. The luminescent image of the TBSL CNT cathode is illustrated in Fig.5(b). It proves that the TBSL CNT cathode fabrication was reliable and feasible for producing a luminescent image. For the backlight sample, the cathode electrons would be accelerated in the vacuum room by the bias voltage. After high-speed cathode electrons bombarded the luminescent layer prepared over the anode substrate-glass, the luminescent image was formed. The illumination of the image pixel in the luminescent image proved that the TBSL CNT cathode could provide a sufficient number of cathode electrons for a practical backlight sample. As seen from the luminescent image, the image pixel in the luminescent image could be illuminated, and the luminous brightness was visible in daylight. This implies that the electron emission current supplied by the TBSL CNT cathode was relatively large, satisfying the needs of running a backlight sample. In the luminescent image, each image pixel's brightness was uniform and nearly the same, which proved the TBSL CNT cathode produced a stable and well-balanced electron emission current.



(a) The fabricated backlight sample with the TBSL CNT cathode (b) Luminescent image of TBSL CNT cathode

Fig.5. Real photos of full-sealed backlight sample

4. Conclusions

The fabrication feasibility studies on the TBSL CNT cathode were performed. A series of low-cost preparation techniques were employed to develop the TBSL CNT cathode. The SiO₂-mixing-layer was fabricated between the emitter-monolayer and bottom-bar-electrode. For the manufacturing process, the repeated-printing + simultaneous sintering method was adopted. The fabricated cathode applied to the backlight sample produced a bright luminescent image, which proved its feasibility and reliability in backlight unit applications. (1) The SEM analysis shows that the prepared TBSL CNT cathode possessed a flat, clean and smooth emitter-monolayer film surface with numerous protruding CNT ends, acting as potential electron sources. (2) Testing of electron emission characteristics of the developed TBSL and reference conducting electrode CNT cathodes proved the former's superiority in terms of a larger electron emission current and a lower turn-on electric field. (3) The emission current stability and emission current measuring repeatability test proved that the TBSL CNT cathode's electron emission was stable and had satisfactory measuring repeatability.

Acknowledgments

This work was supported by the National Natural Science Foundation of China (No.61302167) and the Scientific Research Starting Foundation for High Level Talents in Jinling Institute of Technology (No.jit-rcyj-201602)

References

- [1] Mirko Bacani, Mario Novak, Ivan Kokanovic, et al. Composites of multiwall carbon nanotubes and conducting polyaniline: bulk samples and films produced from a solution in chloroform [J]. *Current applied physics*, 2019, 19(7): 775-779.
- [2] Jennifer A. Rudd, Cathren E. Gowenlock, Virginia Gomez, et al. Solvent-free microwave-assisted synthesis of tenorite nanoparticle-decorated multi-walled carbon nanotubes [J]. *Journal of materials science & technology*, 2019, 35(6): 1121-1127.
- [3] Manishkumar D. Yadav, Kinshuk Dasgupta, Ashwin W. Patwardhan, et al. Controlling the carbon nanotube type with processing parameters synthesized by floating catalyst chemical vapour deposition [J]. *Materialstoday: proceedings*, 2019, 18(3): 1039-1043.
- [4] Lina Marcela Hoyos-Palacio, Diana Paola Cuesta Castro, Isabel Cristina Ortiz-Trujillo, et al. Compounds of carbon nanotubes decorated with silver nanoparticles via in-situ by chemical vapor deposition (CVD) [J]. *Journal of materials research and technology*, 2019, 8(6): 5893-5898.
- [5] Fatih Selimefendigil. Mixed convection in a lid-driven cavity filled with single and multiple-walled carbon nanotubes nanofluid having an inner elliptic obstacle [J]. *Propulsion and power research*, 2019, 8(2): 128-137.
- [6] Azza M. Mazrouaa, Nahla A. Mansour, M. Yahia Abed, et al. Nano-composite multi-wall carbon nanotubes using poly (p-phenylene terephthalamide) for enhanced electric conductivity [J]. *Journal of environmental chemical engineering*, 2019, 7(2): 103002.
- [7] Arjunan Ariharan, Balasubramanian Viswanathan, Vaiyapuri Nandhakumar. Nitrogen-incorporated carbon nanotube derived from polystyrene and polypyrrole as hydrogen storage material [J]. *International journal of hydrogen energy*, 2018, 43(10): 5077-5088.
- [8] Malgorzata Wawrzyniak-Adamczewska. Electronic and magnetic properties of the [4Fe-4S] iron-sulfur clusters encapsulated in a single-walled semiconducting carbon nanotube [J]. *Current applied physics*, 2018, 18(9): 1034-1040.
- [9] Marino Brcic, Marko Canadija, Josip Brnic. Influence of imperfections on double walled carbon nanotube mechanical properties [J]. *Materialstoday: proceedings*. 2018, 5(9): 17397-17403.
- [10] Danial Danaei, Amir Abbas Nourbakhsh, Parvaneh Asgarian, et al. Synthesis of nanosized SiC by low-temperature magnesiothermal reduction of nanocomposites of functionalized carbon nanotubes with MCM-48 [J]. *Ceramics International*, 2019, 45(5): 5525-5530.
- [11] Chidinma Judith Oluigbo, Meng Xie, Nabi Ullah, et al. Novel one-step synthesis of nickel encapsulated carbon nanotubes as efficient electrocatalyst for hydrogen evolution reaction [J]. *International journal of hydrogen energy*, 2019, 44(5): 2685-2693.
- [12] Avwersuoghene Moses Okoro, Ronald Machaka, Senzeni Siphon Lephuthing, et al. Evaluation of the sinterability, densification behaviour and microhardness of spark plasma sintered multiwall carbon nanotubes reinforced Ti6Al4V nanocomposites [J]. *Ceramics international*, 2019, 45(16): 19864-19878.
- [13] Shrilekha V. Sawant, Seemita Banerjee, Ashwin W. Patwardhan, et al. Effect of in-situ boron doping on hydrogen adsorption properties of carbon nanotubes [J]. *International journal of hydrogen energy*, 2019, 44(33): 18193-18204.
- [14] Gwan Woo Kim, Gunn Kim. Behavior of H₂O molecule in carbon nanotube/ boron nitride nanotube heterostructure [J]. *Current applied physics*, 2019, 19(6): 675-678.
- [15] C. S. Martinez, D. E. Igartua, I. Czarnowski, et al. Biological response and developmental toxicity of zebrafish embryo and larvae exposed to multi-walled carbon nanotubes with different dimension [J]. *Heliyon*, 2019, 5(8): e02308.
- [16] Chi-Jung Chang, Yi-Hung Wei, Wen-Shyong Kuo. Free-standing CuS-ZnS decorated carbon nanotube films as immobilized photocatalysts for hydrogen production [J]. *International journal of hydrogen energy*, 2019, 44(58): 30553-30562.
- [17] Amara Arshad, Ayesha Taj, Abdul Rehman, et al. In situ synthesis of highly populated CeO₂ nanocubes grown on carbon nanotubes as a synergy hybrid and its electrocatalytic potential [J]. *Journal of materials*

- research and technology, 2019, 8(6): 5336-5343.
- [18] D. G. Batryshev, Ye. Yerlanuly, T. S. Ramazanov, et al. Influence of dispersion of catalytic carrier for growth mechanism of carbon nanotubes [J]. *Materialstoday: proceedings*, 2018, 5(9): 17447-17452.
- [19] Ekaterina A. Zhukova, Sergey A. Urvanov, Aida R. Karaeva, et al. Longer carbon nanotubes with low impurity level [J]. *Materialstoday: proceedings*, 2018, 5(12): 25948-25950.
- [20] Narasingh Deep, Punyapriya Mishra. Evaluation of mechanical properties of functionalized carbon nanotube reinforced PMMA polymer nanocomposite [J]. *Karbala international journal of modern science*, 2018, 4(2): 207-215.
- [21] G. Satish, V. V. S. Prasad, Koona Ramji. Effect on mechanical properties of carbon nanotube based composite [J]. *Materisaltoday: proceedings*, 2018, 5(2): 7725-7734.
- [22] T. Nagaraj, A. Abhilash, R. Ashik, et al. Mechanical behavior of carbon nanotubes reinforced AA 4032 bimodal alloys [J]. *Materialstoday: proceedings*, 2018, 5(2): 6717-6721.
- [23] Roya Mahinpour, Leila Moradi, Zohreh Zahraei, et al. New synthetic method for the synthesis of 1,4-dihydropyridine using aminated multiwalled carbon nanotubes as high efficient catalyst and investigation of their antimicrobial properties [J]. *Journal of Saudi chemical society*, 2018, 22(7): 876-885.
- [24] Hamzeh Eyni, Hasan Tahermansouri, Farhoush Kiani, et al. Kinetics, equilibrium and isotherms of Pb²⁺ adsorption from aqueous solutions on carbon nanotubes functionalized with 3-amino-5a, 10a-dihydroxybenzo [b] indeno [2,1-d] furan-10-one [J]. *New carbon materials*, 2019, 34(6): 512-523.
- [25] Abdullah Abdulhameed, Nurul Amziah Md Yunus, Izhal Abdul Halin, et al. Simulation of dielectrophoretic alignment for carbon nanotube on indium tin oxide [J]. *Materialstoday: proceedings*, 2019, 7(2): 593-600.
- [26] Han-Seul Kim, Hyungeun Seo, Kyungbae Kim, et al. Facile synthesis and electrochemical properties of carbon-coated ZnO nanotubes for high-rate lithium storage [J]. *Ceramics international*, 2018, 44(15): 18222-18226.
- [27] Vilas G. Dhore, W. S. Rathod, K. N. Patil. Synthesis and characterization of high yield multiwalled carbon nanotubes by ternary catalyst [J]. *Materialstoday: proceedings*, 2018, 5(2): 3432-3437.